Rojava Journal of Science and Technology

2026, VOL. 2, No 1, [16-32]

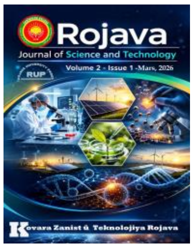

Preparation of an antibacterial Polymeric Membrane Using Nanosilver Extracted from Mulberry Leaves

Haidar Saify Nabiabad[1*], Heba Abdallah[2], Samah A. Hawash[3], Aysel Serdar Ahmed[4]

[1] Department of Biotechnology, Institute of Science and Modern Technology-Rojava University, Syria

[2]Chemical Engineering and Pilot Plant Department, Engineering Research Division, National Research Centre, Egypt

[3] Department of Chemical Engineering, Menoufia Higher Institute of Engineering and Technology, Menoufia, Egypt

[4] Department of Chemical Engineering, Institute of Science and Modern Technology-Rojava University, Syria

Abstract

Ultrafiltration membrane technology is vital for water purification, especially when incorporating nanoparticles due to their unique properties. In this study, anti-fouling and antibacterial membranes were created by blending polyvinyl chloride (PVC) with a silver nanoparticle (AgNP) solution synthesized through an eco-friendly method using mulberry leaf extract. Mixed matrix PVC/AgNP membranes exhibited enhanced properties and performance over the pristine membrane. FTIR and SEM analyses identified functional groups in M1 and M4 and characterized membrane morphology. The manufactured mixed matrix membranes, prepared with 15 wt% PVC and different AgNP wt%, displayed superior mechanical properties compared to the pristine M1. The addition of AgNP solution increased the water uptake capacity of the membranes, as shown by contact angles of 66.1° for the pristine M1 (15% PVC), 54.7° for M4, and 62.7° for M2. Membrane performance improvements were evident, with M1 achieving permeate flux values of 301.4, 314.5, 317.4, 336.9, and 366.4 L/m²·h. M4 exhibited higher flux values of 338.4, 347.4, 354.9, 364.6, and 377.4 L/m²·h during humic acid separation. Bacterial removal tests using Tigris River water showed that M4 achieved a 99.9% removal rate, compared to 58.7% for M1. BOD, COD, and turbidity analyses confirmed M4's superior efficiency in reducing concentrations to 5 mg/L, 7 mg/L, and 0.74 FNU, meeting WHO standards. Fouling resistance tests demonstrated M2's excellent anti-fouling properties, with a flux recovery ratio (FRR) of 99.8%. Therefore, the membrane M2 proves to be an effective anti-fouling.

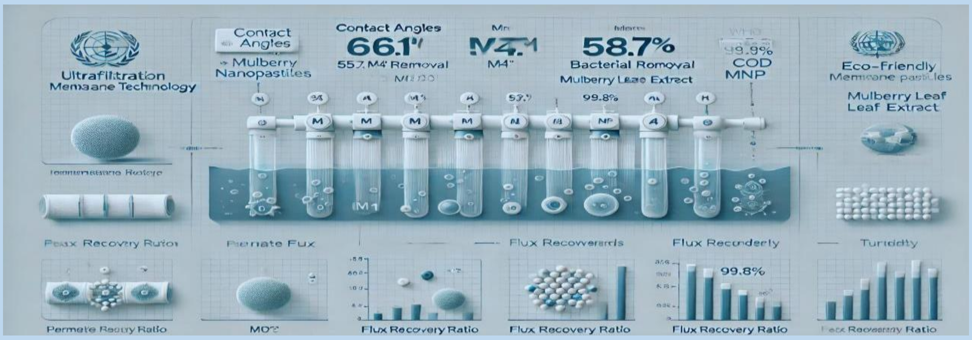

ARTICLE HISTORY
Received 12 Jan. 2025
Revised 3 sept. 2025
Accepted 4 Dec. 2025

Keywords
Ultrafiltration Membrane, Silver Nanoparticles, Polyvinyl Chloride, Tigris River Water, Mulberry Leaf Extract, Antibacterial.

* - Corresponding Corresponding Author: Haidar Saify, homan_saify@yahoo.com

1. Introduction:

Recent advancements in nanotechnology have led to rapid growth in the application of nanoparticles due to their ability to alter or control the molecular properties of materials, enabling the transformation of these materials into structures with desired geometries and characteristics (Cahyana et al. 2021). Among the various methods for synthesizing metallic nanoparticles, chemical approaches are particularly significant. However, these methods typically involve the use of costly and toxic reagents as reducing and stabilizing agents (Halawani 2016). In contrast, biogenic methods for synthesizing metal nanoparticles have gained increasing popularity due to their simplicity, lower toxicity, and eco-friendliness. Metals such as copper, zinc, and silver are frequently used in nanoparticle synthesis because of their notable biomedical properties (Das, Ghosh, and Mandal 2019). Although the biosynthesis of nanoparticles using plant extracts has been well-documented in various species, including neem, Aloe vera, Cinnamomum camphora, Rosa hybrida, and mulberry leaves, the field continues to attract considerable attention due to the vast diversity and high potential of plants as reducing agents, capable of producing nanoparticles with a range of morphologies (Halawani 2016). Silver nanoparticles (AgNPs) are particularly noteworthy, facing an annual demand of approximately 500 tons due to their non-toxic nature, as well as their optical, catalytic, bio-sensing, drug delivery, antioxidant, cytotoxic, and antimicrobial activities (Das, Ghosh, and Mandal 2019). Successful synthesis of AgNPs has been achieved using aqueous extracts from Paronychia argentea Lam. (Alnairat et al. 2021), Ziziphus spina-Christi L. leaves (Cahyana et al. 2021), and Morus alba leaves (Das et al. 2019). The solvents employed in these extraction processes include methanol, ethanol, diethyl ether, chloroform, ethyl acetate, and water. Water-soluble organic compounds present in plant extracts have proven to be potent reducing agents for nanoparticle synthesis (Halawani 2016).Over the past few decades, membrane bioreactor (MBR) technology has been extensively used for the treatment of municipal wastewater and water recycling. MBR systems integrate conventional activated sludge (CAS) processes with membrane filtration, offering advantages such as reduced plant footprint, lower sludge production, and enhanced separation efficiency. However, membrane fouling remains a significant challenge, limiting the broader application of MBRs. The primary cause of membrane fouling in MBRs is biofilm formation on the membrane surface, primarily composed of organic matter and microbial cells. Specifically, the adsorption of natural organic matter (NOM) onto the membrane surface and within its pores results in organic fouling, while bacterial biofilms, typically composed of polysaccharides, form on the membrane surface (Behboudi, Jafarzadeh, and Yegani 2018). Considerable efforts have been made to mitigate fouling through various approaches. It is well-established that membrane characteristics, such as hydrophilicity, surface roughness, and pore size, significantly influence fouling propensity. Enhancing membrane hydrophilicity has beenshown to improve antifouling properties, although some studies have reported contradictory results. To improve hydrophilicity and antifouling performance, various strategies have been employed, including the incorporation of inorganic nanoparticles into polymer matrices, surface modification of membranes, and polymer blending (Behboudi, Jafarzadeh, and Yegani 2018). Polymeric membrane filtration has emerged as a promising technology for producing high-quality, safe reclaimed water, though membrane fouling remains an inevitable issue. Innovative solutions include the development of a novel reactive membrane fabricated through layer-by-layer (LBL) surface modification with polyelectrolytes (PE), followed by the incorporation of anisotropic triangular silver nanoparticles (TSNP) (Ahmad et al. 2019). Additionally, PVC-based hollow fiber ultrafiltration membranes embedded with pristine and modified silver nanoparticles have been prepared using the wet spinning method (Behboudi, Jafarzadeh, and Yegani 2018). These novel membranes exhibit remarkable antibacterial and anti-adhesion properties, achieving a 100% bactericidal effect against high initial bacterial concentrations (10^7 CFU/mL) (Ahmad et al. 2019). Dead-end ultrafiltration (UF) has been identified as a more energy-efficient mode of operation compared to cross-flow filtration for large-scale potable water production (Narendra Kumar et al. 2019). Polymers such as polyvinyl chloride (PVC), polysulfone/silver composites, polyv inylpyrrolidone (PVP), and poly vinylidene fluoride (PVDF) have been commonly used in the manufacture of ultrafiltration membranes.Dead-end ultrafiltration (UF) has been identified as a more energy-efficient mode of operation compared to cross-flow filtration for large-scale potable water production (Chew, Aroua, and Hussain 2018). Polymers such as polyvinyl chloride (PVC), polysulfone/silver composites, polyvinyl pyrrolidone (PVP), and polyvinylidene fluoride (PVDF) have been commonly used in the manufacture of ultrafiltration membranes.

2. Method and Material

2.1 Materials

In preparing silver nanoparticles, several materials were used, such as: mulberry leaves, distilled water, and a 10 mM of silver nitrate solution $AgNO_3$. Polyvinylchloride (PVC) was purchased from Roth India Company. It was used as the main polymer, which was blended with nano-solution that was prepared by Silver nitrate and mulberry leaves. Silver nitrate was purchased from Sigma Aldrich. N-methyl-2-pyrrolidine (NMP) was used as a solvent and polyethylene glycol (PEG 400) was used as a pore former additive, both were purchased from Fluka.

2.2 Preparation of leavies Extract

Silver nanoparticles were synthesized from mulberry leaves because they were the most abundant tree in our regions, and this process was carried out in a number of arranged and detailed steps that were: Fresh mulberry leaves were collected from the tree.these leaves were washed several times with de-ionized water (distilled water) to remove residual debris. Air-dried at ambient temperature for further use.Fifteen grams (15 g) of tinely dissected leaves were boiled with 150 mL deionised water at 90

* - Corresponding Corresponding Author: Haidar Saify, homan_saify@yahoo.com

°C for 45 min. The extract was then lead to cool at ambient temperature.Extract were filtered to eliminate any particles through Whatman filter paper no. 41.

2.3 Synthesis of Silver Nanoparticles (AgNPs

Twenty-five millilitre (15 ml) of leaf extract was added to a solutionof 50 ml, 10 mM of AgNO3. Kept at room temperature with continuous stirring at 250 rpm. The resulting AgNPs were centrifuged to separate them from the supernatant(the bottom layer was contained AgNPs). The remaining unreacted silver was further washed with deionised water and dried at 50 °C for 24 h.

Figure 1: Steps for green synthesis of AgNPs from mulberry leaves, [a] Collect, wash, dry, and chop mulberry leaves, [b] 25 ml of extract with 50 ml of AgNO3 solution, [c]Separation of AgNPs by centrifugation, [d]Separating the two phases by filtration, [e] Drying of AgNPs

2.4 Ultrafiltration Membrane Preparation

The method that was followed in preparing the ultrafilter membrane was the Phase Inversion method by two main steps:

2.4.1 Preparing the membrane mixture/solution

This process is done by mixing the required materials in certain percentages These materials were polyvinyl chloride (PVC) as the main material in the composition of the membrane as a polymeric membrane . Then polyethylene glycol and PEG were added as a pore former . After that, N-methylpyrrolidone (NMP) was mixed as a solvent. These materials are sufficient to make a polymeric ultrafilteration membrane . But what is new here is that a fourth material were blended with the mixture, which was the silver nanoparticles AgNPs that were prepared in the previous steps . This experiment was repeated four times and four membranes were made with different proportions of AgNPs according to the Table (1) below .The polymeric solutions were mixed for 12 hours .Then the solutions were left for 24 hrs to remove bubbles from the polymeric solution.

Table 1: Compositions of additives in each experiment by weight %

Membranes	PVC %	PEG %	NMP%	AgNPs%
M1	15	1	84	0
M2	15	1	83.9	0.1
M3	15	1	83.7	0.3
M4	15	1	83.5	0.5

* - Corresponding Corresponding Author: Haidar Saify, homan_saify@yahoo.com

2.4.2 Ultrafiltration Membrane Preparation

The polyester support was fixed on a glass plate. And membrane film was cast on it using a film applicator with a thickness of 200 µm . Then the glass was immersed on the distilled water coagulation bath.

2.5 Characterizations of Membrane

2.5.1 Scanning Electron Microscope (SEM)

A scanning electron microscope (SEM) was carried out by a QUANTA FEG250 scanning electron microscope apparatus on the membrane's surface and cross-sections. The samples were coated with gold to supply electrical conductivity. The images were conducted at 30 kV (Abdallah et al. 2021).

2.5.2 Mechanical Properties

Mechanical properties for membranes were determined using H5KS universal tensile testing machine. Four specimens per sample with a length of 100 mm, a width of 25 mm, and a thickness of about 0.2 mm were used. The thickness of the samples was measured by a micrometer with an accuracy of 0.01 mm (Abdallah et al. 2021).

2.5.3 Porosity Measurements

Densometers represent one of the accepted standard methods for measuring the porosity and air permeability of membrane. The Gurley Standard Densometer was used to investigate our samples with an area of about 25 cm^2 . The porosity was determined by knowing the weight of the wet sample and of the same sample after drying to reach its stable value. The following equation was used to calculate porosity

$$\varepsilon = \frac{M_w - M_d}{A\,L\,\rho},$$

where A represents the effective area (cm^2), L is the thickness (cm), and ρ the density of pure water(g cm^{-3}). To ensure a minimum error, the calculations were repeated more than five times, and the average value was recorded (Abdallah et al. 2021).

2.5.4 Contact Angle Measurements

Membranes samples contact angles by sessile drop method were measured by a compact video microscope (CVM) that was operated according to the standard test method (ASTM D724-99) of the surface wettability of paper and standard methods (ASTM D5946- 96) of corona- treated polymer films. The volume of droplets on samples was 10µL, where the photo was taken directly after the addition of every drop. An average of three measurements was recorded (Abdallah et al. 2021).

2.5.5 Fourier Transformed Infrared Spectroscopy (FTIR)

FTIR analysis at a resolution of 4 cm^{-1} with 16 scans/min was carried out on membranes samples (M1 & M4) using a Bruker VERTEX 70 FTIR spectrometer equipped. The IR data were determined in the wavenumber range from 400 to 4000 cm^{-1} and a resolution of 4 cm^{-1} (Abdallah et al. 2021).

2.6 Nanosilver characterization

2.6.1 Transmission Electron Microscopy

TEM images were collected at an accelerating voltage of 200 kV. The diameter of the CDs was obtained from the TEM pictures, using Image-Pro Plus software (Some et al. 2020)

Rojava Journal of Science and Technology

2026, VOL. 2, No 1, [16-32]

2.7 Membranes Performance

A laboratory-scale filtration system is composed of a feeding tank, pump, , and dead-end membrane cell as sn. This system was used to indicate the efficiency of the prepared membranes as shown in Figure (1) . The effective area of the membrane in the test cell was 12.56 cm2. First, 0.05 g of humic acid was dissolved in 1 litre Distilled water, membranes was put on membrane cell and tested to indicate the separation percentage and, the analysis was done by UV sepctroscopy apparatus at room temperature (Abdallah et al. 2021). Then, 0.5 g of Boven seruiem Alboumn was dissolved in 1 litre Distilled water membranes was put on membrane cell and tested to indicate the separation percentage.

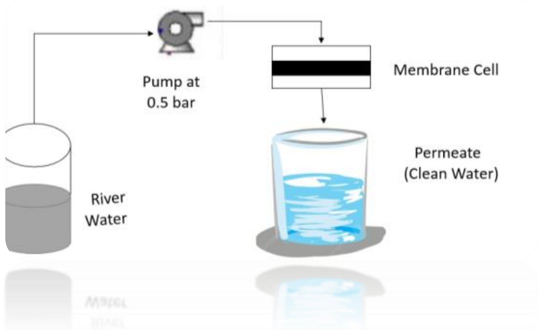

Figure 1: Schematic diagram of the filtration setup

Both the fluxes and separation ratio were calculated using the following equations:

$$Separation\,\% = \frac{C_F - C_P}{C_F} \times 100$$

Where $C_F and\ C_P$ represent the weight fractions in the feed and permeate

respectively of each component.

$$Flux = \frac{V}{Am\ \times t}$$

Where V denote volume of the permeate, measured in liter, Am

is the effective membrane area in square metres, and t is the time in hour.

2.8 Water Sample Collection

Samples were collected from Tigris River, Derik city in Syria, then they were stored at 4 °C. All samples were collected according to the Standard methods for the Water & Wastewater Examination. Tiigris River water contains virus bacterias which were detected in previous research Tiigris River water contains virus bacterias which were detected in previous research (Ologbosere et al. 2016)

2.9 Water Quality Parameters

This study focuses on evaluating specific parameters of river water quality, including bacteria removingoxygen , biological oxygen demand (BOD), chemical xyogen demand (COD), and turbidity.

2.9.1 Microbiological Analysis

Samples were analyzed for microbiological properties immediately after collection. Each analysis was carried out in duplicated and then the mean value was taken. Procedures followed for analysis have been in accordance with the Standard methods for examination of water and wastewater (APHA, 2005). The Total Viable Bacterial Counts (TVBCs) test were determined by using the spread plate method and incubated at 37°C for 24hrs (Ologbosere et al. 2016).

* - Corresponding Corresponding Author: Haidar Saify, homan_saify@yahoo.com

2.9.2 Biological Oxygen Demand (BOD)

BOD is a measure of the organic matter contamination in water, expressed in mg/L. It represents the amount of dissolved oxygen needed for the biochemical decomposition of organic compounds and the oxidation of certain inorganic substances like iron and sulfites (Patil, Sawant, and Deshmukh 2012). BOD is determined according to the Winkler's method, incubation for 5 days at 20°C.

2.9.3 Chemical Oxygen Demand (COD)

COD is another indicator of organic contamination in water, also measured in mg/L. It quantifies the amount of dissolved oxygen required for the chemical oxidation of organic material in water. Both BOD and COD are crucial indicators of the environmental health of surface water, though they are more commonly used in wastewater treatment than in general water treatment. COD is determined using (COD Reactor CR25) as shown in Figure (3-6). (Ologbosere et al. 2016).

2.9.4 Turbidity

Suspended solids in water, like silt and organic matter, increase turbidity and reduce water clarity. This can harm aquatic life by blocking light needed for photosynthesis, lowering dissolved oxygen levels, and raising water temperature. These changes can stress or even kill aquatic organisms, particularly fish, making turbidity an important indicator of water quality and environmental health (Sader 2017). The turbidity of the river water was measured before and after the process for each membrane four times at different times.

2.10 Membrane Fouling Testing

Fouling test was performed by the same performance unit cell using River Water after adding humic acid to the water as a foulant at a ratio of 0.02 g/l. The fouling test was performed on M1, M2, M3 and M4, with the sequence was begun by distilled water for 1 h to determine the permeate fux Jw1 (L/m^2.h) then was followed by the foulant solutions for 2 h to determine the permeate fux Jp (L/m^2.h), and was followed again by distilled water for 1 h to determine Jw2 (L/m^2.h). at room temperature. the permeate fux from membranes was measured Jw2 (L/m^2.h). Fouling parameters were calculated, fux recovery ratio (FRR) was calculated thus)Mansor, Ali, and Shaban 2021(.

$$FRR\% = \frac{J_{W2}}{J_{W1}} \times 100$$

$$Rr\% = (\frac{J_{W2} - J_P}{J_{W1}}) \times 100$$

$$Rir\% = (\frac{J_{W1} - J_{W2}}{J_{W1}}) \times 100$$

$$Rt\% = (1 - \frac{J_P}{J_W}) \times 100$$

Where, (Rr) is the reversible fouling ratio, and (Rir) is the irreversible fouling ratio and Rt% is the total fouling ratio (Mansor et al. 2018).

3. Results and Discussion

* - Corresponding Corresponding Author: Haidar Saify, homan_saify@yahoo.com

3.1. Membrane Characterization

3.1.1. SEM Characterization

Scanning Electron Microscopy (SEM) is commonly utilized to examine the surface and cross-sectional characteristics of polymeric membranes. SEM images of the unmodified PVC membranes' top surface reveal significant details. In Figure (2 a), the membrane exhibits a dense top layer with minute pores visible on the surface. Conversely, Figure (2 b) shows the membrane's top surface with a rougher texture and small, scattered pores. This observation is attributed to the higher concentration of PVC at the film's interface, leading to fewer pores on the membrane's top layer. This phenomenon has also been documented in the literature (Abdallah et al. 2021).

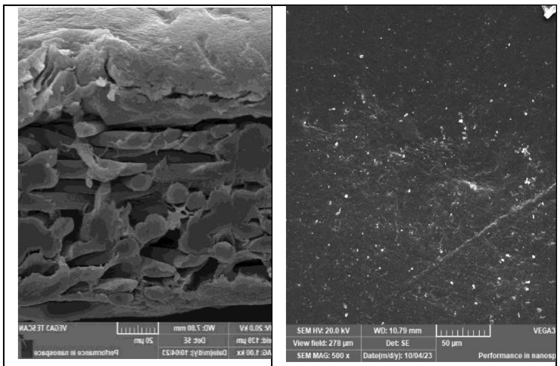

[a] [b]

Figure 2: Shows SEM for M1

Figure (3) illustrates the cross-sectional morphologies of PVC/AgNPs (M2 and M3) membranes fabricated in this study. The images reveal that all the composite membranes exhibit a structure characterized by a broad, finger-like porous sublayer, as seen in the M2 cross-section, and a dense skin top layer—a typical feature of membranes prepared using the non-solvent induced phase separation method. The silver nanoparticles, which contain hydroxyl groups, enhance the exchange between water (non-solvent) and NMP (solvent) during the phase separation process, leading to the formation of larger macrovoids, as observed in M3. Additionally, the backscattered SEM images in Figure (3) show the distribution of nanoparticles throughout the membranes (Abdallah et al. 2021). The M4 membrane demonstrates an impressive structure composed of three distinct layers: a top porous surface, a wide finger-like sublayer with high tortuosity, and a porous bottom layer, which is attributed to the use of a nonwoven support. As shown in Figures (4 a) and (4 b), this structure results from the incorporation of a 0.5 wt% silver nanoparticle solution, which influences the size and shape of the finger-like formations (Abdallah et al. 2021).

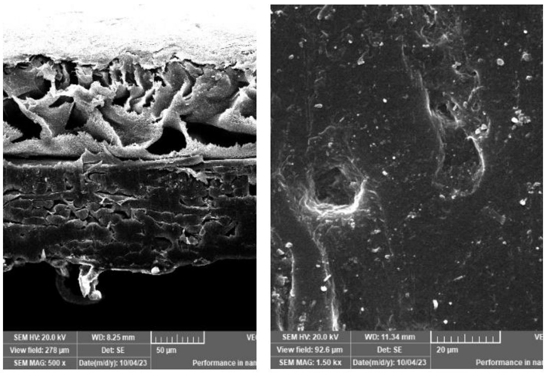

M2 [a] M2 [b]

* - Corresponding Corresponding Author: Haidar Saify, homan_saify@yahoo.com

Rojava Journal of Science and Technology

2026, VOL. 2, No 1, [16-32]

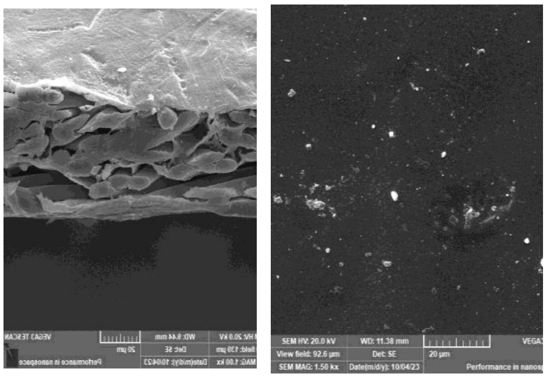

M3 [a] M3 [b]

Figure 3: Shows SEM for M2 and M3

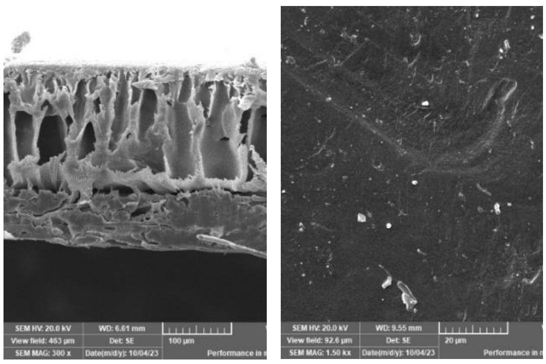

[a] [b]

Figure 4: Shows SEM for M4

3.1.2 Mechanical Properties

The mechanical strength of a membrane is a critical factor that influences its suitability for industrial applications. Figure (5) presents the mechanical test results, which vary according to the percentage of AgNPs in the nano-solution. The results show that M1 has a tensile strength of 26.22 MPa and an elongation of 53.88%, while M2 exhibits a tensile strength of 93.2 MPa and an elongation of 40.92%. In contrast, M3 has a tensile strength of 36.62 MPa with an elongation of 48.97%, and M4 demonstrates a tensile strength of 42.85 MPa with an elongation of 47.58%. The sequence of elongation improvement across the membranes is M1 > M4 > M3 > M2, indicating that M1 has the highest elongation and M2 the lowest. Conversely, the tensile strength order is M2 > M4 > M3 > M1, meaning M2 has the highest tensile strength and M1 the lowest. M3 and M4 exhibit intermediate values in both parameters. The addition of AgNPs has enhanced the tensile strength of the membrane samples, which is likely due to the reinforcing effect of the inorganic additive within the membrane (Behboudi, Jafarzadeh, and Yegani 2018).

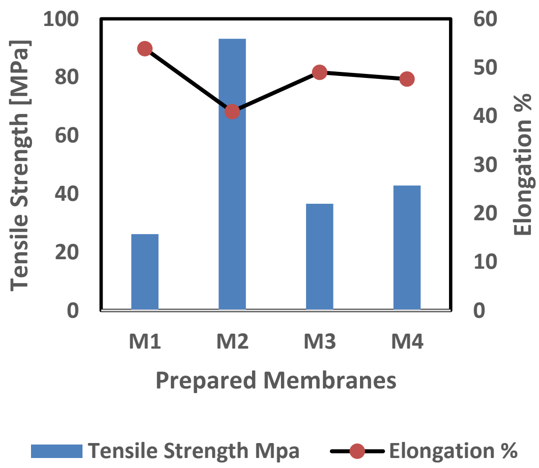

Figure 5: Mechanical properities of Membranes

3.1.3 Contact Angle and Porosity

The increase in the evaporation surface area correlates with the rise in membrane

* - Corresponding Corresponding Author: Haidar Saify, homan_saify@yahoo.com

Rojava Journal of Science and Technology

2026, VOL. 2, No 1, [16-32]

porosity, which in turn leads to higher permeate fluxes. Membrane porosity also influences heat loss through conduction. The porosity levels of the membranes were measured, as shown in Table (2). The porosity of M1 was found to be 71.85%, which is higher than the others. M2 exhibited a porosity of 52%, while M3 and M4 had porosity levels of 16.5% and 14.8%, respectively. It is noteworthy that M4 has the lowest porosity among the membranes, making it a suitable candidate for membrane processes (Bhran et al. 2018).

Hydrophobicity is a critical factor in determining membrane performance, and water contact angle measurements are commonly used to assess the hydrophobicity and wetting properties of membrane surfaces. All membranes were tested using distilled water to measure their contact angles, which were captured using a camera and analyzed by a computer to determine the precise angle. The results, summarized in Table (2), show that M1 has a contact angle of 66.1°, M2 has 62.7°, M3 has 74°, and M4 has 54.7°. These results indicate that M4 has the lowest contact angle at 54.7°, which is attributed to the increased addition of AgNPs. This addition enhances the hydrophilicity of the membrane. The role of AgNPs in the membrane blend includes the production of a porous membrane with uniformly small pores and improved hydrophilic properties of the PVC membrane (Bhran et al. 2018).

Table 2: Values of contact angle and porosity for each membrane

Membrane type	Contact ngle	Porosity %	Wettability image
M1	66.1	61.8	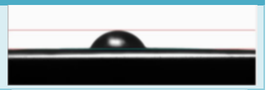
M2	62.7	52	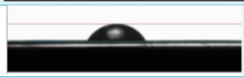
M3	74	16.5	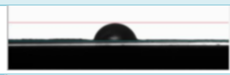
M4	54.7	14.8	

3.1.4 FTIR Characterization

Fourier-Transform Infrared (FTIR) spectroscopy was employed to analyze the distribution of functional groups and molecular orientations within the membranes under study. The FTIR spectrum for M1, which correlates the wavenumber and transmittance for various peaks, is shown in Figure (6). An accompanying table provides the peaks and their intensities, while Table (3) lists the peak wavelengths, the functional groups represented by each peak, and their types. The results indicate that M1 is composed of polyvinyl chloride (PVC) and polyethylene glycol (PEG). The presence of PVC is confirmed by the transmittance peaks at wavenumbers 851.04–969.11 cm^{-1} and 611.62–683.76 cm^{-1}, corresponding to peaks 10 and 11, respectively, which are associated with the characteristic double bonds in PVC. Similarly, the presence of PEG is demonstrated by the double bonds appearing at transmittance peaks 3, 6, and 2, corresponding to wavenumbers 2914.71

* - Corresponding Corresponding Author: Haidar Saify, homan_saify@yahoo.com

cm^{-1}, 1426.16 cm^{-1}, and 3365.51 cm^{-1}, respectively. This evidence confirms that the M1 membrane sample is composed of both PVC and PEG (Kumar et al. 2019).

As previously mentioned, the M4 membrane was created using a blend of PVC, PEG, and AgNPs. The FTIR spectrum for M4, as depicted in Figure (7) and detailed in Table (4), confirms this composition. In addition to the functional groups indicating the presence of PVC and PEG, as described for M1, the FTIR data for M4 suggests the formation of AgNPs through the reduction of Ag^+ ions to Ag^0, as evidenced by peak 11 at 432.14 cm^{-1}. The frequency shifts observed at three specific points—O-H (hydroxyl) at 3365.06 cm^{-1} in peak 2, C≡C (alkyne) at 2326.72 cm^{-1} in peak 4, and $N\text{-}H_2$ (amine) at 3446.46–3819 cm^{-1} in peak 1—indicate that these functional groups are involved in the reduction process. Additionally, the peak around 2909 cm^{-1} corresponds to the stretching of C-H bonds, while the peak at approximately 3365 cm^{-1} is associated with the amide bonds (N-H) of proteins. These functional groups not only facilitate the reduction process but also contribute to the stability of the synthesis (Kumar et al. 2019).

Table 3: Infrated transmittance of M1 resulted by FTIR test

Peak No	Wavenumber cm^{-1}	Bond
1	3751.58	O-H
2	3365.51	O-H
3	2914.71	C-H
4	1730.67	C=O
5	1649.61	C=N
6	1426.16	C-H
7	1328.47	C-N
8	1246.69	C-O
9	1042.47 - 1102.12	C-N or C-O
10	851.04 - 969.11	C-H
11	611.62- 683.76	C-X

* - Corresponding Corresponding Author: Haidar Saify, homan_saify@yahoo.com

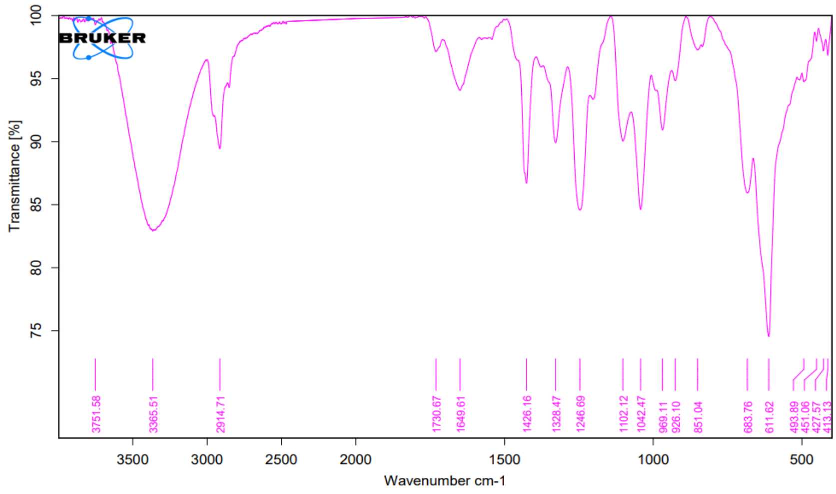

Figure 6: Shows FTIR spectroscopy of M1

Table 4: Infrated transmittance of M4 resulted by FTIR test

Peak No	Wavenumber cm^{-1}	Bond
1	3746.36 - 3819	O-H
2	3365.06	N-H
3	2909.92	C-H
4	2326.72	C≡C
5	1726.9	C=O
6	1550.23	C=C
7	1427.71	C-H
8	1328.47	C-N
9	1245.65	C-O
10	1043.44 - 1099.01	C-N or C-O
11	612.76 - 967.64	C-X
12	432.14	AgNPs(Ag^{+}ion, Ag-ON, ag-H, Ag-O)

* - Corresponding Corresponding Author: Haidar Saify, homan_saify@yahoo.com

2026, VOL. 2, No 1, [16-32]

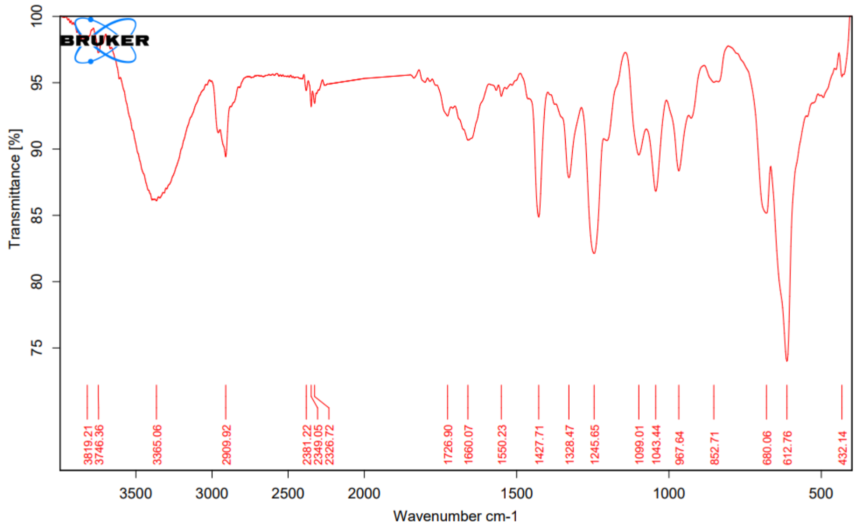

Figure 7: Shows FTIR spectroscopy of M4

3.2 TEM for Nanosilver

Figure 8) illustrates the TEM images of biosynthesized AgNPs were almost spherical, well dispersed, with an average particle size of 6.91 nm, determined from the histogram of particle size distribution, that indicates the crystalline nature of the AgNPs (Some et al. 2020). Agnihotri et al. reported that bioactivity of silver nanoparticles, mainly antimicrobial activity is inversely proportional to the size of the nanoparticles. Present study represents smaller size nanoparticles, supporting their bioactive nature (Agnihotri, Mukherji, and Mukherji 2014).

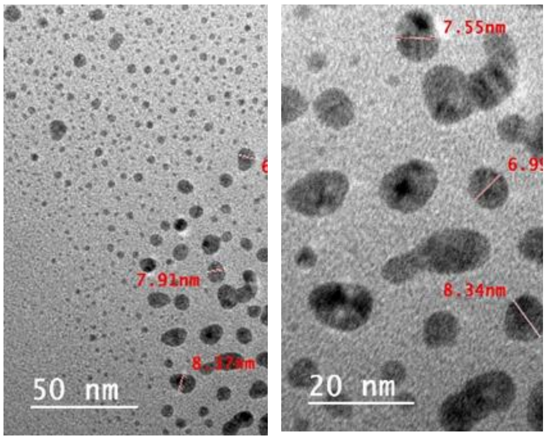

Figure 8: TEM images of nanosilver

* - Corresponding Corresponding Author: Haidar Saify, homan_saify@yahoo.com

Rojava Journal of Science and Technology

2026, VOL. 2, No 1, [16-32]

3.3 Membranes Performance

3.3.1 UV Spectroscopy Analysis of Humic Acid Separation Using Membranes

Figure (9) illustrates the water treatment efficiency in removing humic acid as a function of varying AgNPs percentages. The results show that M3 achieves the highest permeate flux across all percentages compared to M1, which has the lowest permeate flux. This difference is attributed to the presence of 0.3 wt% AgNPs in M3, whereas M1 did not contain AgNPs. Increasing the concentration of the main polymer, particularly when it has a high molecular weight, results in smaller pore sizes. Additionally, a low percentage of pore former leads to reduced porosity and smaller pores, as shown in Table (2). Since AgNPs were not added during M1's preparation, its permeate flux is lower than that of M3, which includes a pore former (PEG) and AgNPs. The addition of silver nanoparticles during membrane preparation also increases the hydrophilicity of the membranes . The results indicate that M3 provides the highest flux compared to other membranes, with a nanosilver concentration of 0.3%, similar to M2 with 0.1% NS. Although M4 has the highest AgNPs concentration at 0.5%, it shows a lower flux compared to M2 and M3, likely due to decreased porosity as a result of the higher AgNPs content. Additionally, using 0.3 wt% NS during membrane formation (M3) facilitates a rapid interchange between the solvent and non-solvent during the coagulation step, leading to the successful and uniform distribution of nanoparticles in the membrane matrix. Consequently, M3 demonstrates the best membrane performance among the tested membranes. However, M4 encounters nanoparticle aggregation issues, leading to reduced homogeneity and increased viscosity of the polymeric solution during preparation. Despite M4 having the lowest contact angle, indicating a highly hydrophilic membrane, these aggregation problems negatively impact its performance (Abdallah et al. 2021).

Figure (9) shows the separation percentage as a function of different AgNPs concentrations. The separation percentage improves as the AgNPs percentage increases. The order of separation efficiency is M3 > M4 > M2 > M1. M1 provides the lowest separation percentage across all feed concentrations compared to other membranes, likely due to its weak selective layer, which diminishes its separation efficiency. The addition of NS to all membranes improvedtheir separation performance (Abdallah et al. 2021). Xie et al developed a novel concept of sequential catalytic ultrafiltration membrane by loading Co3O4/C@SiO2 nanoreactors into finger-like channels for selective separation with peroxymonosulfate-based catalysis to prepare a functional molecular sieve membrane, which showed excellent decontamination performance toward multiple pollutants by filtration of water

* - Corresponding Corresponding Author: Haidar Saify, homan_saify@yahoo.com

matrices containing humic acid (HA) and bisphenol A (BPA). In this study, 100% rejection of HA and 95% catalytic degradation of BPA were achieved under a low pressure of 0.14 MPa and an ultrahigh flow of 229 L/m2/h (Xie et al. 2021).

3.3.2 Boven Seruiem Alboumn Removing

Figure (10) illustrates the water treatment efficiency in removing boven seruiem alboumn as a function of varying AgNPs percentages. The results show that M1 achieves the highest permeate flux across all percentages compared to M3, which has the lowest permeate flux. This difference is attributed to the presence of 0.3 wt% AgNPs in M3, whereas M1 contains no AgNPs. Since AgNPs were not added during M1's preparation, its permeate flux is higher than that of M3, which includes a pore former (PEG) and 0 wt% AgNPs. Although M4 has the highest AgNPs concentration at 0.5%, it shows a lower flux compared to M1, likely due to decreased porosity as a result of the higher AgNPs content. Consequently, M1 demonstrates the best membrane performance among the tested membranes. However, M2, M4, and M3 encounters nanoparticle aggregation issues, leading to reduced homogeneity and increased viscosity of the polymeric solution during preparation, these aggregation problems negatively impact its performance.

Figure (10) shows the separation percentage as a function of different AgNPs concentrations. The separation percentage improves as the AgNPs percentage increases. The order of separation efficiency is M2 > M3 > M4 > M1. M1 provides the lowest separation percentage across all feed concentrations compared to other membranes, likely due to its weak selective layer, which diminishes its separation efficiency. The addition of NS to all membranes improvedtheir separation performance (Abdallah et al. 2021). Membranes fabricated by Ilyas et al. were made from superhydrophilic and anticorrosive polyvinyl chloride based on graphene oxide-silver (GO-Ag) nanolayers. The water flux and bovine serum albumin rejection of the pure polyvinyl chloride membrane were improved from 192 lm-2 h-1 to 613 lm-2 h-1 and 81.5% to 92.1%, respectively (Ilyas et al. 2021).

* - Corresponding Corresponding Author: Haidar Saify, homan_saify@yahoo.com

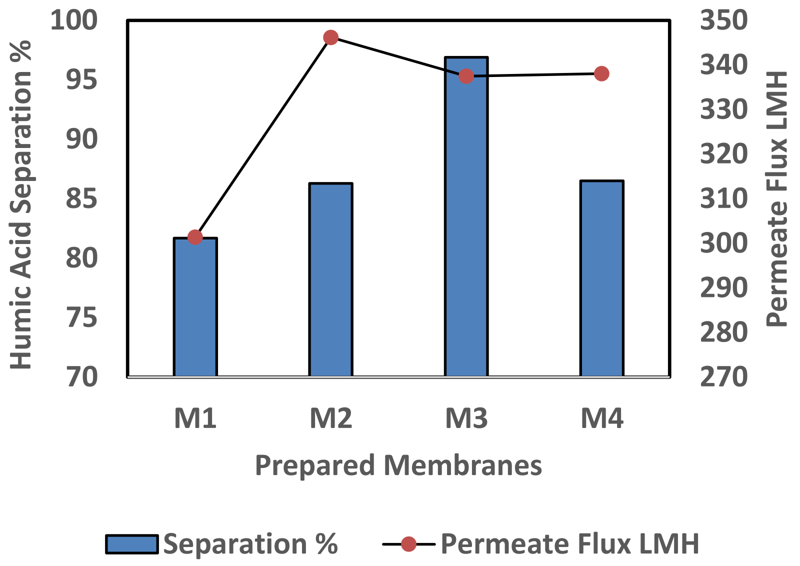

Figure 9: Humic acid separation percentage using PVC/Mn(acac)3 membranes.

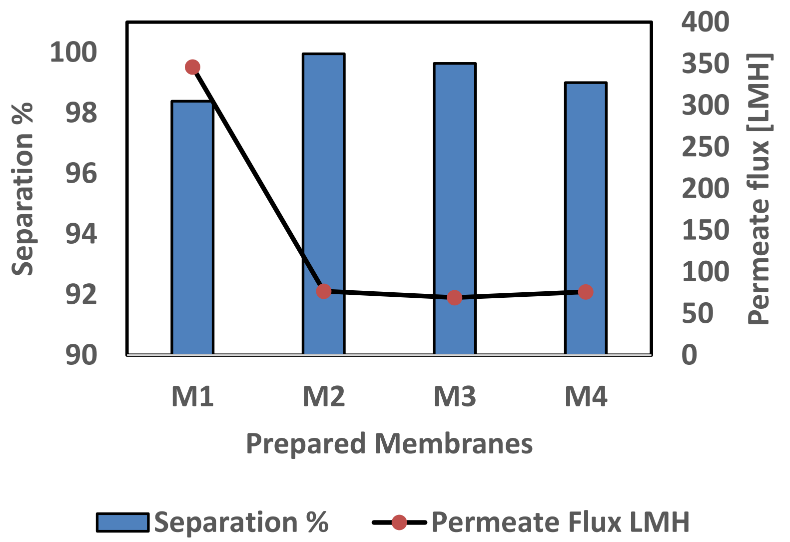

Figure 10: Boven seruiem alboumn separation percentage using PVC/Mn(acac)3 membranes

3.4 Water Quality Parameters

3.4.1 Bacteria Removing from Tigris River

The river water contains many bacteria, the river water sample was tested on the membrane filtration system. Table (5) shows the significance of viruses in the river water before and after treatment with membranes. The results indicate that bacteria were detected with a value of 5150 CFU/100 ml before the membrane. While after the membrane, the concentration of bacteria removed by each membrane decreases as follows from the most concentrated to the least concentrated in the order M1 > M2 > M3 > M4.

Table 5: River water quality parameters before and after treatment and comparison with standard river water criteria

Name	Bacteria (CFU/100 ml)	Turbidity (FNU)	BOD (mg/l)	COD (mg/l)
Standard (Juwana et al. 2022)	<100	<5	<3-5	<10-15
River Water	5150	30.6	44	144
M1 (0 AgNPs)	2127.75	5.6	26	64
M2 (0.1 AgNPs)	56.5	0.94	17	46
M3 (0.3 AgNPs)	3.5	0.8	9	21
M4 (0.5 AgNPs)	0.5	0.79	5	7

M4 (consisting of 0.5% AgNPs solution) has a negative detection of almost all viruses (0.5 CFU/100ml), which means that the M4 membrane separates all viruses from the river water. The M1 membrane (0% AgNPs solution) separates bacteria with a value of 2128 CFU/100ml, perhaps because the pores of this membrane have a large size compared to other membranes that contain the AgNPs nanosilver, which depends on separating viruses through a sieving mechanism. While M2, M3, and M4 contain AgNPs in their structure which exhibit excellent bacterial removal, silver atoms in the nano NS solution eliminate bacteria, like a vaccine in the body, by oxidizing the amino acid residues of the protein envelope of viruses (Abdallah et al. 2021). AgNPs can break the protein structure of viruses due to the high oxidation capacity of these nanoparticles with proteins, which can destroy the virus. Therefore, the addition of these particles in the membrane fabrication can provide a disinfection membrane against any virus (Abdallah et al. 2021). Figure (11) shows permeate flux and separation % of membranes, where M2 provides the highest flux 55.8 L/m^2.h. While M4Achieved the highest separation 99.9% for bacteria removing. Ahmed et al reported the first ever successful attempt to fabricate a novel anti-fouling reactive membrane by layer-by-layer (LBL) surface modification with polyelectrolyte (PE), followed by anisotropic triangular silver nanoparticles (TSNPs). The novel membrane exhibited antibacterial and antiadhesive properties by achieving 100% bactericidal effect against

* - Corresponding Corresponding Author: Haidar Saify, homan_saify@yahoo.com

high initial bacterial concentration (107 CFU mL1) (Ahmad et al. 2019).

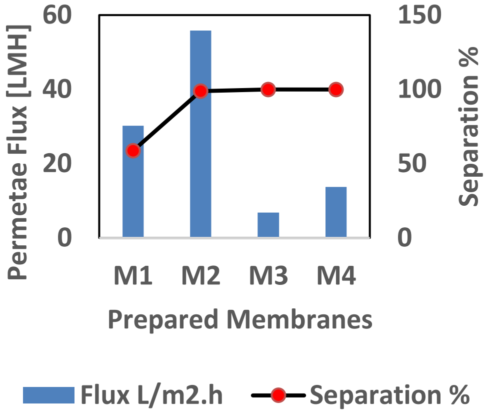

Figure 11: Bacteria separation percentage using PVC/Mn(acac)3 membranes

Da Silva et al prepared PVC nanocomposites with silver nanoparticles (AgNPs) in the molten state. PVC/silver nanocomposites showed virucidal activity against SARS-CoV-2 (strain B.1.1.28) within 48 h when the silver content was at least 0.3% (da Silva et al. 2023)

A study by Zhu and Lua showed that silver nanoparticles impregnated with PES membrane surfaces were 100% effective in killing various marine bacteria and bacteria in seawater collected off Sentosa Island, Singapore. These membranes have excellent antibacterial and antifouling properties that can be used to kill bacteria in ballast water and seawater (Zhu and Lua 2021).

3.4.2 BOD and COD Measurement

Table (5) also shows the results of measuring both BOD and COD for river water before and after dinner, where the BOD concentration before the membrane was 44 mg/l, while the COD concentration was 144 mg/l, which are large values that exceed the permissible limits according to the standard criteria for water quality set by ISO, so the membranes should be tested to determine their capabilities in separating these two criteria. After the membrane, it was found that M1 has an excellent separation ratio because it does not contain AgNPs, while we note that with an increase in the percentage of AgNPs wt%, the separation efficiency increases and the concentration of both BOD and COD decreases, due to the antibacterial and antipollution properties of silver nanoparticles (Ologbosere et al. 2016).

3.4.3 Turbidity Measurement

The river water sample was tested on the membrane filtration system to measure the turbidity value, where Table (5) shows the turbidity value in the river water before and after treatment with membranes. The results indicate a turbidity value of 30.6 FNU before the membrane. That is, in untreated water, and this result is close to the results obtained by Jabar and Hassan (Jabar and Hassan 2022). While after the membrane, the turbidity value removed by each membrane decreases as follows from

* - Corresponding Corresponding Author: Haidar Saify, homan_saify@yahoo.com

the most concentrated to the least concentrated in the order M1 > M2 > M3 > M4. M4 (consisting of 0.5% AgNPs solution) has a turbidity value of 0.79 NFU, which is less than the permissible limits for international water quality standards. This means that the M4 membrane for removing turbidity from river water is excellent. The M1 membrane (0% AgNPs solution) separates turbidity with a value of 5.66 CFU, which is slightly higher than the standards set by the World Health Organization. Perhaps because the pore size of this membrane is large compared to other membranes containing nano NS solution, which also relies on turbidity separation through screening mechanism. While M2, M3, and M4 contain AgNPs in its structure which shows excellent removal of turbidity of river water.

3.5 Membrane Fouling Test

High reversible resistance over irreversible resistance means the membrane can be easily washed, where the reversible resistance depends on the formation of foulants cake on the membrane surface without clogging the pores, so it can be removed by surface or backwash. Irreversible resistance means the pores were clogged by foulant and this case needs chemicals or backwash under pressure, which increases the cost of the process and reduces the lifetime of the membrane (Liu, Zhu, and Xu 2007).

Figure (12) illustrates that the membranes exhibit antifouling behavior, where the results indicate that washing of the membrane surface after using humic acid solution many times provides the ability to use membranes again.

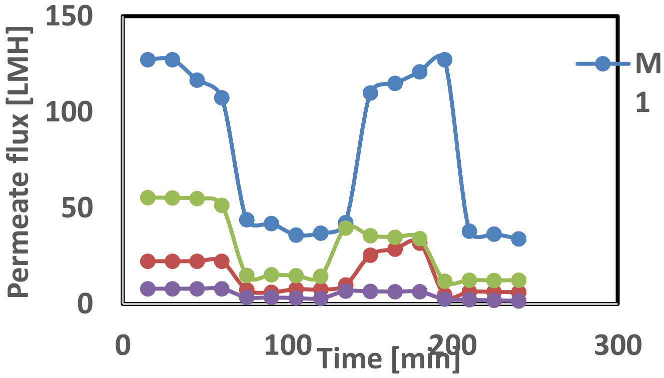

Figure 12: Fouling test using prepared membranes M1, M2, M3, and M4

The results indicate that Rr was 51.8% for M1, 79.4% for M2, 68.2% for M3, and 50.7% for M4. Irreversible resistance Rir was 13.6% for M1, 0.63% M2, 2.22% for M3, and 17% for M4. However, the FRR for M1 was 86.4 %, 97.8% for M2, 97.77% for M3, and 83% for M4 as shown in Figure (13). It can be observed that the irreversible resistance of M2 was very low that makes this membrane super antifouling. Using AgNPs with PEG enhances the membrane hydrophilicity and antifouling membrane surface as shown in M2, that because the negative charge and paramagnetic properties of AgNPs can make electrostatic charge between the membrane surface and humic acid solution. According to that, M2 has too low irreversible resistance compared with other membranes, which means M2 is a super-antifouling membrane that can be used in wastewater treatment. These laboratory results are the nucleus for producing this

* - Corresponding Corresponding Author: Haidar Saify, homan_saify@yahoo.com

Rojava Journal of Science and Technology

2026, VOL. 2, No 1, [16-32]

type of membrane (PVC/AgNPs on rarge scale to be applied in pilot units as ultrafiltration spiral wound modules or large flat sheet membranes to be used as a membrane for wastewater treatment. After the success of the pilot test. The membranes can be produced in the form of an industrial scale to be applied in the wastewater plants (Abdallah et al. 2021).

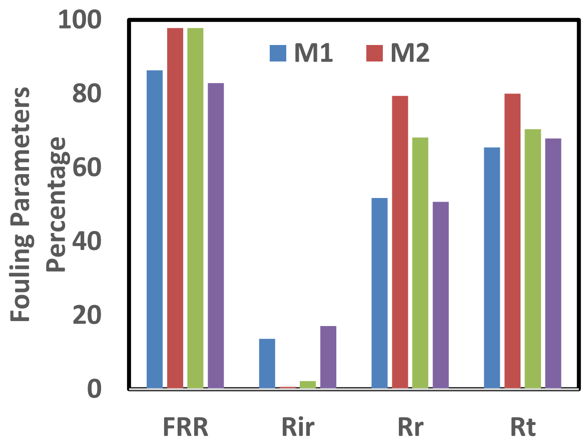

Figure 13: Fouling resistance & FRR using prepared membranes

Membrane M4, with the highest concentration of AgNPs, exhibited outstanding antibacterial efficacy, effectively reducing bacterial concentrations to a minimum in comparison to the other membranes. However, M2 demonstrated superior anti-fouling performance. This contrast can be attributed, in part, to the low porosity of M4 (14.8), which results in a reduced flux and subsequently a lower flux recovery rate (FRR) relative to M2. Additionally, M4's enhanced ability to remove biochemical oxygen demand (BOD), chemical oxygen demand (COD), and turbidity leads to the accumulation of these contaminants within its pores. This accumulation increases the irreversible resistance (Rir%) while contributing to M4's lowest reversible resistance (Rr%) among the tested membranes.

Maleki et al. (2024) studied nanoparticles from organometallic cultures of U-66-NH2 and preparation of carbonaceous biochar from pyrolysis of Cladophora glomerata algae as novel modifiers and used them to manipulate mixed matrix polyethersulfone (PES) membranes. Through fouling experiments with humic acid and bovine serum albumin, only 12.9 and 34% reduction in water fluxes were recorded for the best performing modified membrane (Maleki and Bozorg 2024).

Soundarrajanet al. (2023) investigated the separation of bovine serum albumin using a novel mixed membrane composed of polyvinylpyrrolidone and poly(phenylene ether ether sulfone)/nano-silver. The anti-fouling properties of the mixed matrix membranes were evaluated. The flux recovery ratio of PEES/PVP/Nano-Silver membranes was 97%, which was much higher than that of PEES/Nano-Silver membranes (62%) (Soundarrajan et al. 2023).

4. Conclusion

1. Silver nanoparticles (AgNPs) were successfully synthesized using mulberry leaf extract and a silver nitrate solution,

* - Corresponding Corresponding Author: Haidar Saify, homan_saify@yahoo.com

achieving an efficient, eco-friendly, and cost-effective approach.

2. Various PVC mixed matrix membranes were prepared via phase inversion using different ratios of the nanosolution (NS).

Among the membranes, M2 exhibited the highest tensile strength at 93.2 MPa, while M1 provided the greatest elongation percentage at 53.88%.

3. The addition of NS% to all membranes improved their hydrophilicity and reduced porosity, enhancing the separation efficiency. Specifically, M4 (0.5 wt% AgNPs) had the lowest porosity at 14.8% compared to other membranes.

4. FTIR analysis was conducted to confirm that the membranes were composed of the stated materials, identifying functional groups based on their specific wavelengths. Analysis was performed on membranes M1 and M4, revealing that M1 consisted of PVC and PEG, while M4 contained NS%.

5. SEM analysis was carried out on the four membranes to examine the surface and cross-sectional characteristics of the polymeric membranes. Images indicated that all composite membranes displayed a finger-like porous substructure, and SEM micrographs showed the distribution of nanoparticles throughout the membranes. TEM images of biosynthesized AgNPs were almost spherical, well dispersed, with an average particle size of 6.91 nm, determined from the histogram of particle size distribution, that indicates the crystalline nature of the AgNPs .

6. In terms of membrane performance, concerning flow rate and separation efficiency, M2 showed the highest permeate flux at 346.2 L/m².h for humic acid removal, while M3 achieved the highest separation efficiency at 96.9%. For bovine serum albumin (BSA) removal, M2 demonstrated the highest separation efficiency at 99.5%, while M1 exhibited the highest flux at 363.4 L/m².h.

7. The membranes were applied in the treatment and purification of Tigris River water, with M4 being the most effective in removing bacteria, turbidity, BOD, and COD.

8. The M4 membrane, with the highest AgNP concentration, excels in turbidity and bacterial removal but shows high irreversible resistance due to low porosity and contaminant accumulation. In contrast, the M2 membrane demonstrates superior antifouling and reusability, making it more suitable for efficient wastewater treatment.

Thus, the research questions were addressed, proving that membranes containing silver nanoparticles demonstrate significant anti-fouling and antibacterial properties compared to pure polymeric membranes, with these properties increasing as the NS% rises.

Acknowledgments

The authors would like to thank the Institute of Science and Modern

* - Corresponding Corresponding Author: Haidar Saify, homan_saify@yahoo.com

Technology (ISMT), and the University of Rojava in North and East Syria, for their financial support and all the facilities they provided to complete this work.

References

Abdallah, Heba, Marwa Shalaby, Li-Feng Fang, Bao-Ku Zhu, and Ahmad Shaban. 2021. "Mixed Matrix Membranes from Polyvinylchloride and Manganese Organic Complex Compound for Fouling and Viral Resistance." *Journal of Membrane Science and Research* 7 (3):196-208.

Agnihotri, Shekhar, Soumyo Mukherji, and Suparna Mukherji. 2014. "Size-controlled silver nanoparticles synthesized over the range 5–100 nm using the same protocol and their antibacterial efficacy." *Rsc Advances* 4 (8):3974-3983.

Ahmad, Jabran, Xianghua Wen, Fengjuan Li, and Bo Wang. 2019. "Novel triangular silver nanoparticle modified membranes for enhanced antifouling performance." *RSC advances* 9 (12):6733-6744.

Alnairat, Nour, Muna Abu Dalo, Rund Abu-Zurayk, Saida Abu Mallouh, Fadwa Odeh, and Abeer Al Bawab. 2021. "Green synthesis of silver nanoparticles as an effective antibiofouling material for polyvinylidene fluoride (PVDF) ultrafiltration membrane." *Polymers* 13 (21):3683.

Behboudi, A, Y Jafarzadeh, and R Yegani. 2018. "Enhancement of antifouling and antibacterial properties of PVC hollow fiber ultrafiltration membranes using pristine and modified silver nanoparticles." *Journal of Environmental Chemical Engineering* 6 (2):1764-1773.

Bhran, Ahmed, Abeer Shoaib, Doaa Elsadeq, Ayman El-gendi, and Heba Abdallah. 2018. "Preparation of PVC/PVP composite polymer membranes via phase inversion process for water treatment purposes." *Chinese journal of chemical engineering* 26 (4):715-722.

Cahyana, Antonius Herry, Agus Rimus Liandi, Yoki Yulizar, Yoga Romdoni, and Tio Putra Wendari. 2021. "Green synthesis of CuFe2O4 nanoparticles mediated by Morus alba L. leaf extract: Crystal structure, grain morphology, particle size, magnetic and catalytic properties in Mannich reaction." *Ceramics International* 47 (15):21373-21380.

Chew, Chun Ming, Mohamed Kheireddine Aroua, and Mohd Azlan Hussain. 2018. "Advanced process control for ultrafiltration membrane water treatment system." *Journal of cleaner production* 179:63-80.

da Silva, Daniel J, Guilherme B Gramcianinov, Pamela Z Jorge, Vanessa B Malaquias, Augusto A Mori, Mário H Hirata, Sergio AM Lopes, Luciano A Bueno, Mathilde Champeau, and Danilo J Carastan. 2023. "PVC containing silver nanoparticles with antimicrobial properties effective against SARS-CoV-2." *Frontiers in Chemistry* 11:1083399.

Das, Dipayan, Raja Ghosh, and Palash Mandal. 2019. "Biogenic synthesis of silver nanoparticles using S1 genotype of Morus alba leaf extract: characterization, antimicrobial and antioxidant potential assessment." *SN Applied Sciences* 1:1-16.

Halawani, Eman Mohamed. 2016. "Rapid biosynthesis method and characterization of silver nanoparticles using Zizyphus spina christi leaf extract and their antibacterial efficacy in therapeutic application." *Journal of*

* - Corresponding Corresponding Author: Haidar Saify, homan_saify@yahoo.com

Biomaterials and Nanobiotechnology 8 (1):22-35.

Ilyas, Hafsa, Abdul Haleem, Muzaffar Iqbal, and Muhammad Siddiq. 2021. "Influence of GO-Ag nano-filler on the antibacterial, antifouling and hydrophilic characteristics of polyvinyl chloride membrane." *Journal of Water Process Engineering* 44:102336.

Jabar, Shaimaa Satar, and Fikrat M Hassan. 2022. "Monitoring the Water Quality of Tigris River by Applied Overall Index of Pollution." IOP Conference Series: Earth and Environmental Science.

Kumar, Brajesh, Karla Sofía Vizuete, Vishal Sharma, Alexis Debut, and Luis Cumbal. 2019. "Ecofriendly synthesis of monodispersed silver nanoparticles using Andean Mortiño berry as reductant and its photocatalytic activity." *Vacuum* 160:272-278.

Liu, Fu, Bao-Ku Zhu, and You-Yi Xu. 2007. "Preparation and characterization of poly (vinyl chloride)-graft-acrylic acid membrane by electron beam." *Journal of applied polymer science* 105 (2):291-296.

Maleki, Amin, and Ali Bozorg. 2024. "Biochar decorated with metal–organic framework nanoparticles as robust modifier to manipulate nanofiltration mixed matrix membranes characteristics and performance." *Chemical Engineering Journal* 490:151564.

Mansor, Eman S, Eman A Ali, and AM Shaban. 2021. "Tight ultrafiltration polyethersulfone membrane for cheese whey wastewater treatment." *Chemical Engineering Journal* 407:127175.

Mansor, Eman S, Tarek S Jamil, Heba Abdallah, and AM Shaban. 2018. "Highly thin film nanocomposite membrane based metal organic complexes for brackish water desalination." *Journal of environmental chemical engineering* 6 (4):5459-5469.

Narendra Kumar, HK, N Chandra Mohana, BR Nuthan, KP Ramesha, D Rakshith, N Geetha, and Sreedharamurthy Satish. 2019. "Phyto-mediated synthesis of zinc oxide nanoparticles using aqueous plant extract of Ocimum americanum and evaluation of its bioactivity." *SN Applied Sciences* 1:1-9.

Ologbosere, OA, HSA Aluyi, AG Ogofure, A Beshiru, and FAECAL I Omeje. 2016. "Physico-chemical and microbiological profile of bacterial and fungal isolates of Ikpoba River in Benin City: Public health implications." *African Journal of Environmental Science and Technology* 10 (3):67-76.

Patil, PN, DV Sawant, and RN Deshmukh. 2012. "Physico-chemical parameters for testing of water–A review." *International journal of environmental sciences* 3 (3):1194-1207.

Sader, Mike. 2017. "Turbidity measurement: A simple, effective indicator of water quality change." *OTT Hydromet. Retrieved from http://www. ott. com/en-us/products/download/turbidity-white-paper*.

Some, Sudip, Biraj Sarkar, Kinkar Biswas, Tushar K Jana, Debjoy Bhattacharjya, Paulami Dam, Rittick Mondal, Anoop Kumar, Apurba K Deb, and Abdul Sadat. 2020. "Bio-molecule functionalized rapid one-pot green synthesis of silver nanoparticles and their efficacy toward the multidrug resistant (MDR) gut bacteria of silkworms (Bombyx mori)." *RSC advances* 10 (38):22742-22757.

Soundarrajan, M, Khuloud A Alibrahim, J Krishnamurthi, P Maheswari, A Harikrishnan, Abdullah Alodhayb, and MR Muthumareeswaran. 2023.

* - Corresponding Corresponding Author: Haidar Saify, homan_saify@yahoo.com

"Preparation, enhancement of permeability, and anti-biofouling properties of PEES/nano-silver/PVP mixed-matrix membrane." *Materials Research Express* 10 (1):015301.

Xie, Wancen, Alberto Tiraferri, Xuanyu Ji, Chen Chen, Yuhua Bai, John C Crittenden, and Baicang Liu. 2021. "Green and sustainable method of manufacturing anti-fouling zwitterionic polymers-modified poly (vinyl chloride) ultrafiltration membranes." *Journal of Colloid and Interface Science* 591:343-351.

Zhu, Jianhua, and Aik Chong Lua. 2021. "Antibacterial ultrafiltration membrane with silver nanoparticle impregnation by interfacial polymerization for ballast water." *Journal of Polymer Science* 59 (20):2295-2308.

* - Corresponding Corresponding Author: Haidar Saify, homan_saify@yahoo.com